Formation of Silver Nanoparticles in Deoxyribonucleic Acid−Poly(*o*-methoxyaniline) Hybrid: A Novel Nano-biocomposite

Arnab Dawn and Arun K. Nandi*

Polymer Science Unit, Indian Association for the Cultivation of Science, Jadavpur, Kolkata 700 032, India

Received: May 27, 2006; In Final Form: July 26, 2006

A novel nano-biocomposite of silver and poly(*o*-methoxy aniline) (POMA)/DNA hybrid has been prepared by adding DNA solution to an aqueous solution of POMA (emeraldine base, EB) and $AgNO_3$ mixture. The mixture was aged for 10 days and was freeze-dried to form the hybrid nanocomposite (weight fraction of DNA = 0.75). FESEM pictures show a fibrillar network morphology of the biomolecular hybrid with silver nanoparticles on its surface. The TEM picture also corroborates silver nanoparticle formation in the biomolecular hybrid, and the denser population of nanoparticles in the TEM micrograph as compared to that in the SEM micrograph indicates that the nanoparticles are present inside the fibrils in greater proportion. The dc conductivity value of the hybrid indicates that POMA (EB) is doped by silver ion and the doped POMA form complexes with DNA through electrostatic interaction of the radical cation of POMA (emeraldine salt form, ES) and the DNA anion. During the doping process and Ag nanoparticle formation, a fluctuation of the π band to polaron band transition peak occurs together with a complementary fluctuation of the polaron band to π^* band transition peak. After 53 h of aging, the former shows a slow but continuous red shift with aging time. This has been attributed to the slow uncoiling of POMA on the DNA surface. The conformation and crystal structure of DNA remain intact during the nano-biocomposite formation. The dc conductivity value of the nano-biocomposite is almost the same as that of the pure POMA−DNA hybrid at the same composition, but the I−V characteristic curve of the nano-biocomposite is somewhat different showing an insulating region on low applied voltage. At higher applied voltage, it shows a semiconducting property characterizing the large band gap semiconducting behavior of the nano-biocomposite.

Introduction

In recent years, the self-assembly of metal nanoparticles to form well-defined nano-structured materials has received considerable research interest. For this purpose, DNA is widely recognized as an ideal candidate for assisting the bottom-up assembling of nanostructures. It has recently been demonstrated that metal nanoclusters can be formed through a DNA templated process that uses the chemical reduction of DNA-complexed metal ions.[1] One-dimensional parallel and two-dimensional crossed palladium nanowires,[2] copper nanowire,[3] and silver nanorod[4] were fabricated on DNA template with direct reduction of metal ion. Recently, Wei et al. synthesized silver nanoparticles, nanorods, and nanowires on the surface of DNA network.[5] By controlling the pore size of the DNA network, silver nanoparticles, nanorods, and nanowires were produced without using any surfactant. DNA templated nanowires of silver,[6] platinum,[7] palladium,[8] etc. are also reported from the chemical reduction of DNA-complexed metal ion. Recently, gold nanoparticle−DNA conjugates having a specific number of long double-stranded DNA strands were prepared by gel electrophoresis.[9]

Electronically conducting polymers are important materials, and composites of these materials with metal nanoparticles have also drawn significant research attention in recent years. The family of composites may have the conducting component either dispersed in inorganic matrix or it may incorporate the other phase.[10] Polyaniline (PANI) is an important member of the conducting polymer family, and its nanocomposites with gold nanoparticles are well studied.[11,12] The nanocomposite is used to detect DNA hybridization. Apart from gold, PANI/Ag nanocomposite formation is reported by Khanna et al.[13] by mild photolysis of silver salt in aqueous aniline by UV radiation. The nanocomposites of PANI/Pt[14−16] and PANI/Pd[17−19] have been studied in detail for their electrocatalytic properties and sensing applications. The chemical system of PANI−Au nanocomposite with intact electronic property of PANI was recently achieved by Kinyanjui et al.[20] Apart from the polyaniline, the nanocomposites of other members of the conducting polymer family are well studied. For example, Pinter et al.[21] reported the preparation and properties of a conducting polypyrrole−chloride/nitrate-nanosized silver composite. Conducting polymers have been successfully applied as the conducting part of composite materials with Fe_2O_3,[22] V_2O_5,[23] CdS,[24] and most of the works deal with the nanoparticles of noble metals (Pd, Pt, Au).[25−27]

Various kinds of applications are found with such materials, such as biological and biomedical applications,[28,29] nanoparticle-based molecular switches,[30] nanodevices,[31] nanocircuitries,[6] etc. These wide applications are due to the fact that the size of the nanoparticle is reduced to the length scale of a few nanometers, the same as that of the mean free path of electrons in the material. This exhibits properties different from those of the bulk material of the same compositions,[32] and this quantum size effect has an influence on their optical, electronic, magnetic, and catalytic properties.[33−35] Thus, new materials with new properties may be produced from these important nanocom-

* Corresponding author. E-mail: psuakn@mahendra.iacs.res.in.

10.1021/jp063269z CCC: $33.50 © 2006 American Chemical Society
Published on Web 08/29/2006

posites. Silver nanoparticles are of great interest because of their use in surface enhanced Raman spectroscopy,[36] catalysis,[37,38] etc. Different methods have been used for the preparation of silver nanoparticles, and they include microemulsions,[39] Langmuir−Blodgett films,[40] thermal decomposition,[41] and biosynthesis using biological organisms.[42]

In this Article, we shall explore the possibility of a DNA−conducting polymer hybrid for the preparation of Ag nanoparticles. From the above survey, it is clear that both conducting polymers and DNA separately produce nanocomposites with noble metals. However, special techniques are required for such nanocomposite preparation in these individual systems. Here, we explore utilization of the combined properties of DNA and conducting polymer to produce the Ag-nanocomposite. It is now established that polyaniline is easily doped with transition metal ions.[43] Metal ions with lower standard reduction potential values (Ni^{2+}, Cu^{2+}, etc.) form complexes with the amine nitrogen of PANI. These complexes produce bipolarons and polarons by oxidation under atmospheric oxygen in the PANI chain, thereby making it conducting. Ag^{+}/Ag has a higher standard reduction potential than that of Ni^{2+} and Cu^{2+}, so it may get reduced easily in the process to metallic Ag. If there is any stabilizer in the medium, it may become stabilized as the nanoparticle of silver. DNA may act as a good stabilizer of nanoparticles for its ionomeric property. So the DNA−conducting polymer hybrid may be useful in preparing Ag nanoparticles. Earlier, we reported the preparation and properties of conducting polymer−DNA hybrids with intact conformation and structure of DNA using the water-soluble poly(*o*-methoxyaniline).[44−46] Here, we report a method similar to that to prepare a composite of Ag nanoparticle with the above biomolecular hybrid. Such a composite is expected to find use in various biosensing applications.

Experimental Section

Samples. Calf thymus DNA (Type 1; sodium salt) was purchased from Sigma Chemicals. POMA was synthesized in the laboratory from the monomer, *o*-methoxy aniline, in 1 M HCl medium in the presence of 5.8 M LiCl using ammonium peroxydisulfate.[44] The molar ratio of reactants was 1.0:4.3:39.6 for ammonium peroxydisulfate, *o*-methoxy aniline, and 1.0 M HCl, respectively. They were mixed at −35 °C, and the reaction mixture was stirred for 2 days at −18 °C. The polymer was collected by filtration and washed repeatedly with double distilled water. The emeraldine (EB) base form of POMA was obtained by stirring it with 0.1 M ammonium hydroxide solution for 48 h and then was dried in a vacuum. The viscosity average molecular weight was found to be 20 900.[44] The $AgNO_3$ (G. R. grade) sample was purchased from E. Merck India and was used as received. All of the experiments were done in sterilized triple distilled water.

Preparation of Hybrid Composite of Silver. An aqueous solution of POMA (EB) (0.005% w/v) was made by sonicating in an ultrasonic bath (60 W, model AVIOC, Eyela) for half an hour, and a transparent blue solution was obtained. The hybrid composite of silver was prepared by adding 15 mL of a 0.02% aqueous solution of Na−DNA to an aqueous solution containing a mixture of 20 mL of 0.005% POMA (EB) and 0.5 mL of N/1000 $AgNO_3$ solutions (mixed for 1 h). Thus, in the reaction mixture the weight ratio is 1:3 for POMA (EB) and Na−DNA, respectively. The concentration of silver ion in the reaction medium was 1.41×10^{-5} M. The sample was aged for 10 days and was then freeze-dried. The hybrid solution and the dried sample were stored under a dark cover in a closed environment.

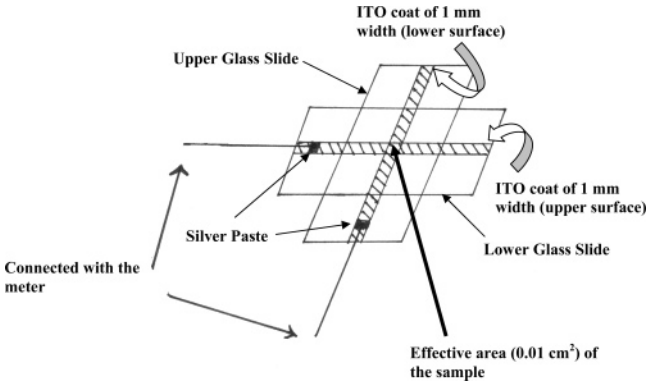

Figure 1. Sandwiching of nano-biocomposite sample between two ITO-coated glasses in the ITO method for the conductivity measurement.

Microscopy. The scanning electron microscopy was done by dropping one drop of the solution aged for 10 days on a microscopic cover slip and dried in air and finally in a vacuum at room temperature (30 °C). It was then platinum coated and observed in a field emission scanning electron microscope (FE-SEM), JEOL, JSM-6700F.

The transmission electron microscopy (TEM) study was done by dropping a drop of its dilute solution (aged for 10 days) on a carbon-coated copper grid and then drying at room temperature in air and finally in a vacuum at 30 °C. It was then observed in a high-resolution transmission electron microscope, JEOL, 2010EX, operated at an accelerated voltage of 200 kV fitted with a CCD camera. The electron diffraction experiment was carried out on a nanoparticle observed in the TEM micrograph, and the crystal spacing (d_{hkl}) values were calculated directly by measuring the distance between the opposite spots on the same circumference of the diffraction pattern using the software of the instrument.

Circular Dichroism (CD) Spectra. CD spectra of the aqueous solutions of POMA (EB), Na−DNA, and Ag−hybrid composite were done in a spectropolarimeter (JASCO, J-600) in a 1 cm quartz cuvette. It was scanned from 700 to 200 nm at 30 °C.

UV−Vis Spectra. UV−vis studies were done in aqueous solution in a quartz cell of thickness 1 cm for the wavelength range 190−1100 nm in a UV−vis spectrophotometer (Hewlett-Packard, model 8453) at 30 °C. Pure water spectrum was subtracted from the solution spectra. The UV−vis spectra of the hybrid composite solution were taken at different aging times.

FT-IR Spectra. The FT-IR spectra of the samples were done in a Nicolet FT-IR instrument [Magna IR-750 spectrometer (series-II)]. Solid samples were mixed with KBr, and pellets were made to run the scan.

Wide Angle X-ray Scattering (WAXS) Study. The WAXS studies of Na−DNA, Ag−hybrid composite, and POMA (EB) were performed in a diffractometer (Philips, PW 1830). Nickel filtered Cu Kα radiation was used in the work. The samples were taken in powder form, and the scan was made at the step size of 0.02° 2θ with time per step = 0.5 s.

Conductivity Measurement. The dc conductivity of the samples was measured by the two-probe method in nitrogen atmosphere to avoid the effect of atmospheric moisture on the conductivity. The conductivity was measured by sandwiching the sample between two ITO conducting strips of 1 mm width placed perpendicularly (Figure 1). The thickness of the sample was measured using a screw gauge and was 0.019 cm. The area of the sample was 0.01 cm^2. The conductivity of the sandwiched

sample was measured by an electrometer (Keithley, model 617) at 30 °C using the following equation:

$$\sigma = \frac{1}{R} \times \frac{l}{a} \quad (1)$$

where l is the thickness, a is the area of the sample, and R is the resistance.

The ITO method of measuring conductivity was checked with the conductivity of a poly(3-hexylthiophene) film by the standard two-probe method. The ITO method exhibits a conductivity of 4.2×10^{-9} S/cm, whereas the latter method exhibits a conductivity of 6.8×10^{-9} S/cm, indicating the suitability of the ITO method for such conductivity measurement. The I−V characteristics of Ag−hybrid composite were studied using the same sample by applying voltage from −5 to +5 V, and the current was measured at each applied voltage. The voltage was varied by an increment rate 0.2 V in 12 s (i.e., 1 V/min) from −5 to + 5 V, and the current (I) was measured at each step.

Results

Microscopy (SEM). We shall discuss here the morphology of the Ag−POMA/DNA nanocomposite with a weight fraction of DNA = 0.75 in the POMA/DNA hybrid. This composition of the hybrid is chosen as it shows optimum physical properties, for example, well-defined UV−vis spectra, maximum doping characteristics, and stable Ag nanoparticle formation. The FE-SEM picture of the hybrid nanocomposite is presented in Figure 2a, and fibrillar network morphology is observed for the POMA−DNA hybrid where silver is present as silver nanoparticle. The silver nanoparticles are clearly seen in the enlarged portion of the box in Figure 2a that is presented in Figure 2b. As the morphology of the nanocomposite of the biomolecular hybrid is fibrillar and also homogeneous, it indicates that POMA and DNA mix well in the process and the hybrid produces the fibril. Figure 2b clearly presents that there are Ag nanoparticles on the surface of the fibrils. The presence of Ag nanoparticles inside the fibrils cannot be judged from FE-SEM experiment because FE-SEM deals with the surface morphology. The nanoparticles observed on the fibril surface may be of metallic Ag as evidenced from the EDXS picture (Figure 2c). A close examination of Figure 2b reveals that there are different sizes of Ag nanoparticles ranging from 20 to 250 nm in diameter.

To understand the correct distribution of Ag nanoparticles in the fibrils of the hybrid, a TEM picture of the above sample is presented in Figure 3a. Here, silver nanoparticles are distributed as darker spots on lighter contrast hybrid material, and they are of different sizes with a wider distribution of sizes. The population of Ag nanoparticles in the TEM micrograph is denser than that observed in the FE-SEM picture (Figure 2b). This indicates that the Ag nanoparticles are present inside the fibrils in larger density than that on the surface. In Figure 3b, the electron diffraction pattern of a nanoparticle of the micrograph (Figure 3a) is shown. From the diffraction pattern, the crystal spacing (d_{hkl}) values are calculated and compared to the ASTM data of metallic Ag in Table 1. The data definitely indicate that the nanoparticles are of metallic Ag.[47]

Circular Dichroism (CD) Spectroscopy. In Figure 4, the CD spectra of the Ag−POMA−DNA nanocomposite solution in water are presented with those of the component spectra. POMA has a positive peak at 211 nm, whereas Na−DNA has positive peaks at 219 and 278 nm and a negative peak at 248 nm. In the composite, the peaks of Na−DNA are fully retained, indicating that the double helical structure of DNA hybrid remains intact in the process of nanocomposite formation. Thus,

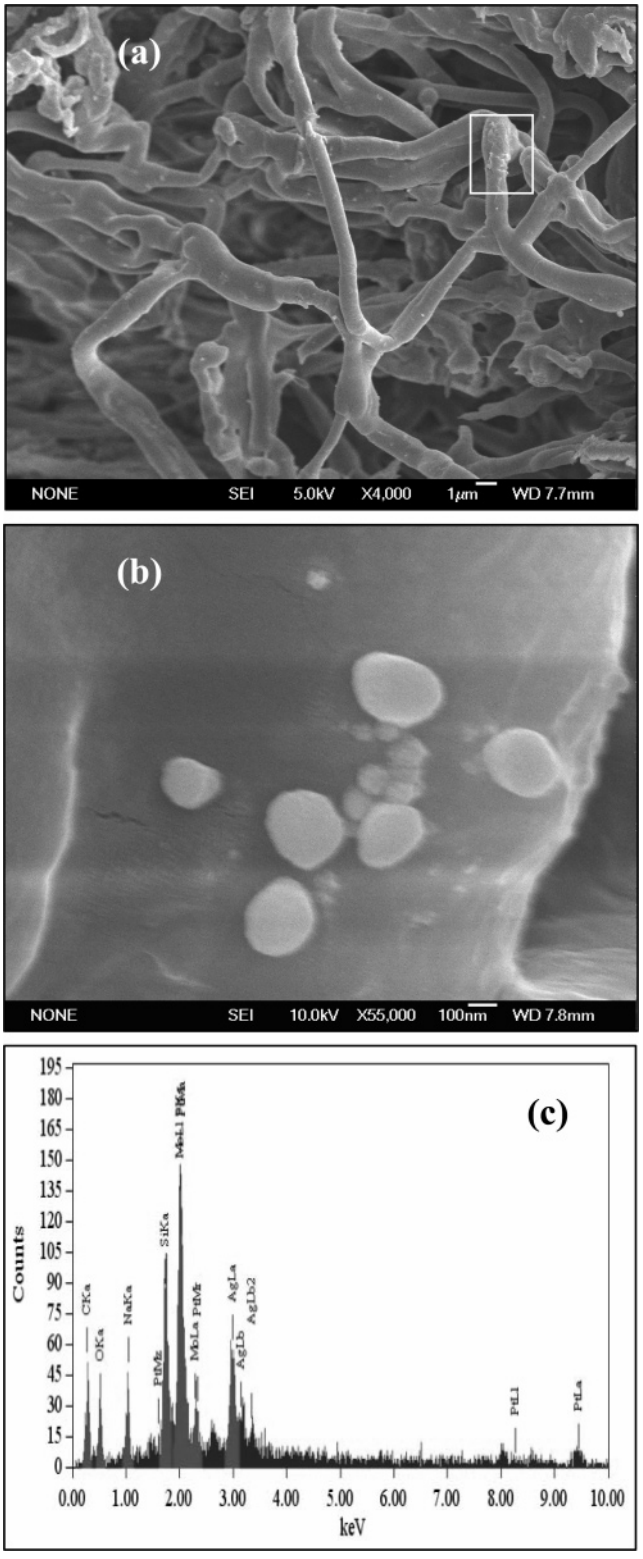

Figure 2. (a) SEM micrograph of Ag-nano-biocomposite, (b) magnified picture of its marked portion, and (c) EDXS pattern of the SEM image.

in the reaction of Ag^+ with POMA−DNA mixture, no conformational change of DNA occurs. However, some conformational change of POMA might occur as the intensity of the 220 nm peak of the hybrid remains the same as that of Na−DNA and no contribution for POMA helicity is observed. Thus, it may be concluded that during the Ag nanoparticle formation the DNA double helical structure remains intact, which is similar to that during the formation of the pure POMA−DNA hybrid.[44−46]

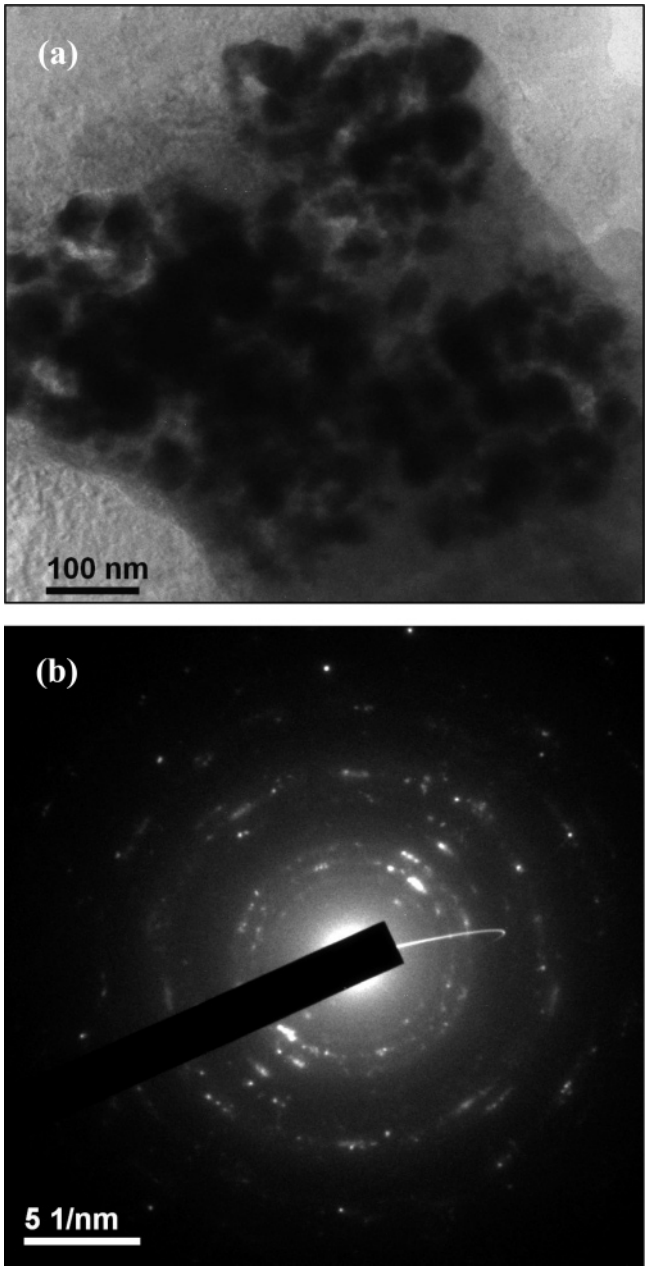

Figure 3. (a) TEM micrograph of the Ag-nano-biocomposite, and (b) electron diffraction pattern of the nanoparticle of the micrograph (a).

TABLE 1: Comparison of d_{hkl} Values Calculated for the Ag-Nano-biocomposite from Electron Diffraction Experiment with that of Metallic Silver

d_{hkl} calculated (Å)	d_{hkl} ASTM (Å)
2.38	2.36
1.98	2.04
1.44	1.44
1.23	1.23
1.15	1.18

X-ray Diffraction Study (WAXS). In Figure 5, the WAXS pattern of the hybrid nanocomposite is compared to those of Na−DNA and POMA. It is apparent from the figure that the DNA structure in the hybrid nanocomposite remains intact. Thus, it may be concluded that the DNA crystal structure remains intact even in the silver nanoparticle formation from the mixture of Na−DNA, $AgNO_3$, and POMA solutions. This observation is also similar to that of pure POMA−DNA hybrid formation where the DNA crystal structure was intact.[44−46]

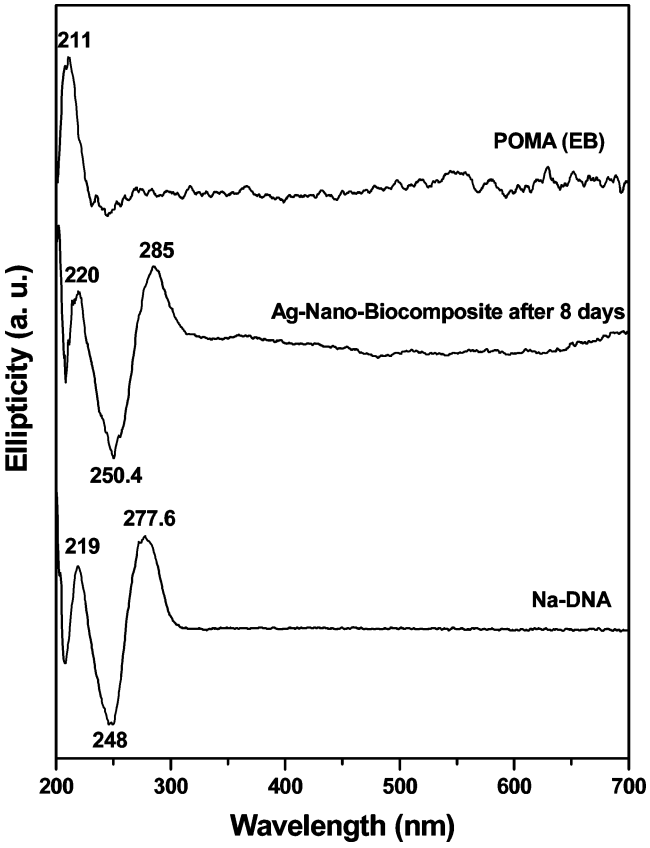

Figure 4. CD spectra of POMA (EB), Ag-nano-biocomposite, and Na−DNA solutions at 30 °C.

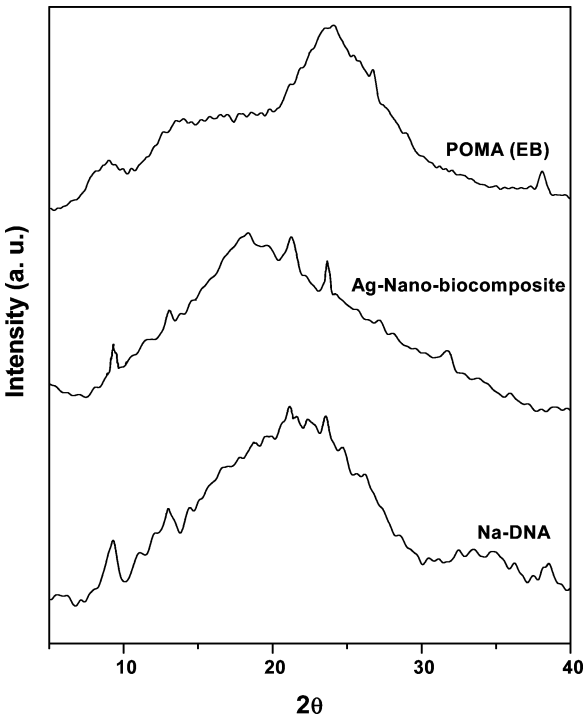

Figure 5. WAXS patterns of POMA (EB), Ag-nano-biocomposite, and Na−DNA.

UV−Vis Spectra. In Figure 6a,b, the UV−vis spectra of the system are shown for different aging times. The peak at 262 nm (Figure 6a) corresponds to the transition of the base pair of Na−DNA, and it remains the same in both intensity and peak position as that of pure Na−DNA. This peak also remains invariant with aging time. The 321 nm peak (Table 2) corre-

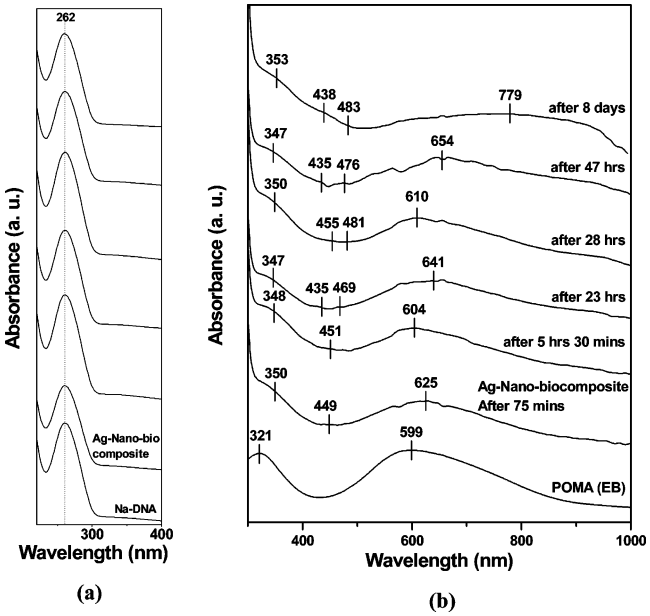

Figure 6. UV−vis spectra of POMA (EB), Na−DNA, and Ag-nano-biocomposite for different aging times at 30 °C: (a) portion of UV−vis spectra showing DNA peak positions in the nano-biocomposite, and (b) portion of UV−vis spectra showing POMA peak positions in the nano-biocomposite.

TABLE 2: Peak Positions of Ag-Nano-biocomposite at Different Aging Times in the UV−Vis Spectra

aging time	transition for base pair in Na-DNA (nm)	$\pi-\pi^*$ transition (nm)	polaron band−π^* band transition (nm)	plasmon band of silver nanoparticle (nm)	π band−polaron band transition (nm)
75 min	262	350	449		625
5 h 30 min	262	348	451		604
23 h	262	347	435	469	641
28 h	262	350	455	481	610
47 h	262	347	435	476	654
53 h	262	350	436	480	639
3 days	262	349	435	480	669
4 days	262	351	438	481	697
6 days	262	350	440	482	718
7 days	262	352	439	483	756
8 days	262	353	438	483	779
9 days	262	353	438	483	779

sponds to the $\pi-\pi^*$ transition of POMA (EB), which changes to 350 nm after 75 min of complexation with DNA and $AgNO_3$ solution. Such a shift of $\pi-\pi^*$ transition of POMA usually occurs when it is doped with protonated DNA.[44−46] Thus, it may be argued that $AgNO_3$ is doping POMA (EB) as Na−DNA has no capacity to dope POMA (EB). A hump at 449 nm is newly generated and may be attributed to the polaron band to π^* band transition.[48] It fluctuates initially with time, but after 47 h it is almost invariant. The most important observation is that the 599 nm peak of POMA (EB) (electronic excitation band of benzonoid to quinonoid ring[48−50]) disappears and a new peak appears at 625 nm. This may be attributed to the π band to polaron band transition peak, which initially fluctuates, and after 53 h of aging it shows a gradual red shift with time. Finally, it levels off at 779 nm after a week. This initial fluctuation followed by a continuous red shift of the π band to polaron band transition is very interesting for this system. The fluctuations of both the transitions are better represented in Figure 7. It may be noted that the fluctuation of the polaron band to π^* band transition (lower curve) is complementary with the π band to polaron band transition (upper curve); that is, when there is

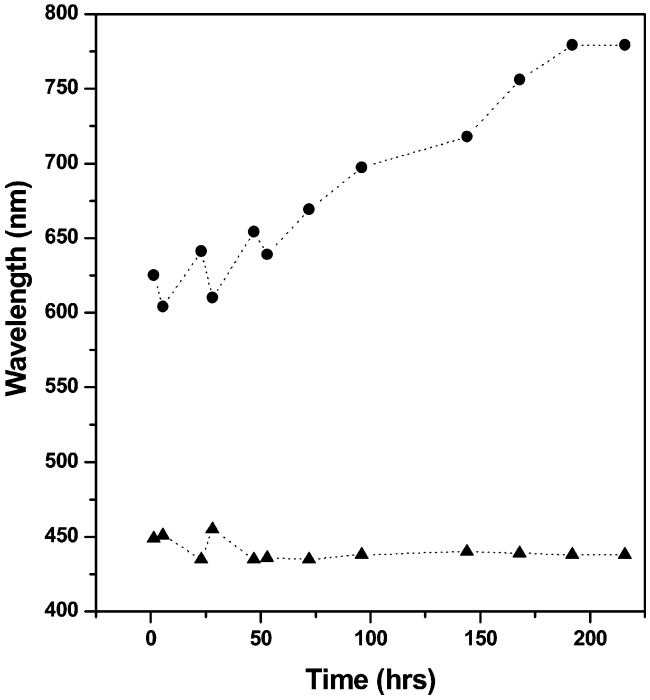

Figure 7. Plot of the peak positions for the π band to polaron band transition (●) and polaron band to π^* transition (▲) with aging times in the UV−vis spectra.

a blue shift in the former transition peak, there is a red shift in the later transition peak, particularly at the initial stage of doping. These fluctuations of the π band to polaron band and polaron band to π^* band transition were found to be reproducible for the three sets of experiments performed by us.

In POMA−DNA hybrid, we previously reported the slow red shift of the π band to polaron band transition with increasing aging time due to the uncoiling of POMA chain on the DNA surface.[44−46] In the present system, the uncoiling occurs due to electrostatic repulsion between the radical cations produced due to the doping of POMA by Ag^+. This repulsive interaction within the POMA chain becomes stable due to the large molecular weight of DNA where POMA gets adsorbed during the doping process. This uncoiling of POMA chain increases the conjugation length of the molecule, causing a slow red shift of the π band to polaron band transition. The cause of fluctuation of the π band to polaron band transition peak at the initial stage is not totally clear and may be related to the doping by Ag^+ followed by silver nanoparticle formation. The initial fluctuation of the polaron band to π^* band transition is due to the same reason as in the π band to polaron band transition, and these will be addressed in the Discussion. It may be noted that at about 23 h of aging a small peak at ∼469 nm appears (Figure 6), and it may be attributed to the plasmon band of Ag nanoparticles.[51,52] This band is red shifted to a small extent with time (Table 2) probably due to the increased size of Ag nanoparticles.

FT-IR Spectra. In Figure 8, the FT-IR spectra of POMA, Na−DNA, and the hybrid nanocomposite are presented. It is apparent from the figure that almost all of the component peaks are present in the FTIR spectra of the hybrid. POMA (EB) has a prominent peak at 1115 cm^{-1}, which may be correlated with the 1160 cm^{-1} peak of polyaniline (PANI, EB), corresponding to a vibration mode of quinonoid (Q) structure (N═Q═N) with partial electronic-like character.[53,54] The lower peak position as compared to that of PANI may be due to the conjugation of the lone pair of electrons of the *o*-OCH_3 group with the double

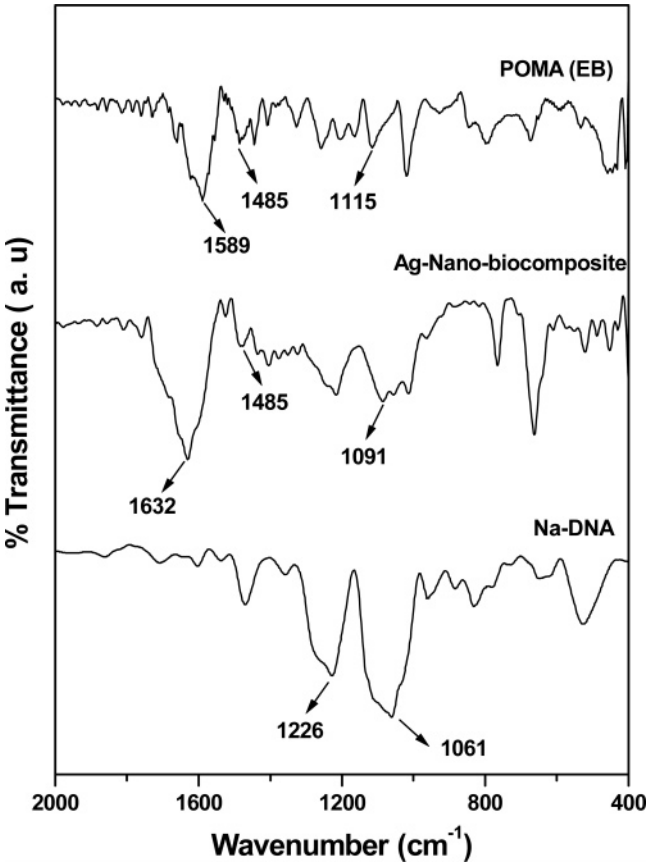

Figure 8. FT-IR spectra of POMA (EB), Ag-nano-biocomposite, and Na−DNA.

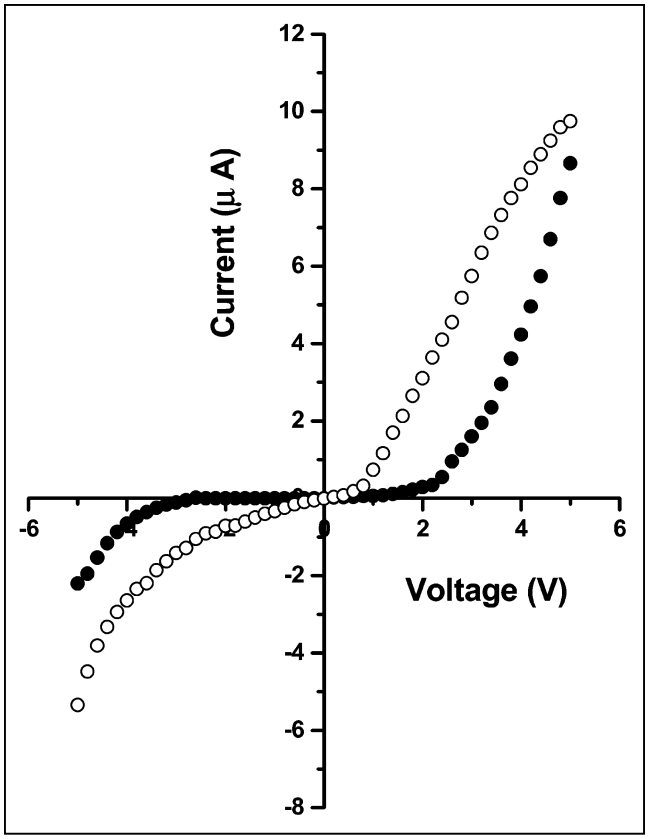

Figure 9. Comparison of I−V characteristics of the Ag-nano-biocomposite (●) and the POMA (EB)−DNA (protonated) (W_{DNA} = 0.71) hybrid (○).

bonds of quinonoid ring decreasing the bond order. On doping by Ag^+, this band further shifts to the lower frequency region (1091 cm^{-1}) due to the loss of double bond character by polaron formation (B−N^+•H−B, B = benzonoid ring). From a comparison of POMA spectra with the hybrid spectra, it is apparent that the 1589 cm^{-1} peak shifts to 1632 cm^{-1}. The 1589 cm^{-1} peak is due to the quinonoid ring deformation,[54] and it shifts to higher energy 1632 cm^{-1} due to the formation of a rigid (i.e., unconjugated) quinonoid structure of POMA (pernigraniline base, PB). The 1485 cm^{-1} peak of POMA (EB) is for the deformation of benzonoid ring, and it remains almost unchanged in the hybrid. It is important to note that the relative intensity of quinonoid deformation with respect to that of benzonoid ring increases in the hybrid nanocomposite more than that of POMA (EB). This indicates that quinonoid ring population increases relative to that of benzonoid structure in the hybrid. Thus, from this IR study, it may be concluded that some change in benzonoid structure of POMA (EB) is occurring due to the formation of hybrid silver nanocomposite.

Conductivity Measurement. The dc conductivity of the hybrid nanocomposite was measured at 30 °C and was found to be 3.2×10^{-6} S cm^{-1}. The order of conductivity is the same as that of the DNA−POMA (EB) biomolecular hybrid with similar composition (2.9×10^{-6} S cm^{-1}).[45] These results clearly indicate that the Ag^+ ion dopes POMA (EB) well and the conductivity arises due to the doping of POMA. Na−DNA has no contribution to this conductivity as discussed in our earlier reports.[44−46] In Figure 9, the I−V characteristic curve of the hybrid nanocomposite is compared to that of pure POMA−DNA hybrid (W_{DNA} = 0.71) at 30 °C. It is apparent from the figure that there is some difference in the nature of the two I−V curves. At low voltage, the hybrid nanocomposite I−V curve shows apparently no change, characterizing more insulating behavior than that of the POMA−DNA hybrid. However, at higher voltage, it shows a sharper increase, indicating large band gap semiconducting behavior of the hybrid nanocomposite. Although Ag is conducting in the bulk form, the presence of silver nanoparticle in the hybrid nanocomposite may be responsible for this semiconducting behavior. The above I−V behavior of the nano-biocomposite is found to be independent of scanning rate and scanning direction (Supporting Information Figure 1).

Discussion

We will now discuss how the Ag nanoparticles are produced. It is well known that metal ions can dope polyaniline and its derivatives.[43,55] Therefore, it is reasonable to consider that POMA is doped well by the Ag^+. A probable mechanism of such doping is presented in Scheme 1.[43] Because of the higher value of standard reduction potential of silver ion (+0.8 V), it forms complexes with amine nitrogen atoms of POMA (EB) (Scheme 1a).[43,56] The complex is then oxidized, producing bipolaron in one chain and transferring the other chain into the pernigraniline (PB) base form (Scheme 1b). Because of the production of PB, the blue shift of the π band to polaron band transition occurs. On further aging, it transforms into a complex with a delocalized polaron in one chain and the PB form of the other chain (Scheme 1c). This increases the conjugation in the POMA chain, and as a result a red shift occurs in the π band to polaron band transition. With further aging, Ag^+ gets reduced forming metallic Ag separating the PB chain from the polaron chain. The mechanism of transformation of complexed Ag^+ into metallic Ag is not yet clear to us. Probably excess POMA (EB) slowly reduces complexed Ag^+ into metallic Ag and itself transforms into the PB form. Such a situation causes another

SCHEME 1

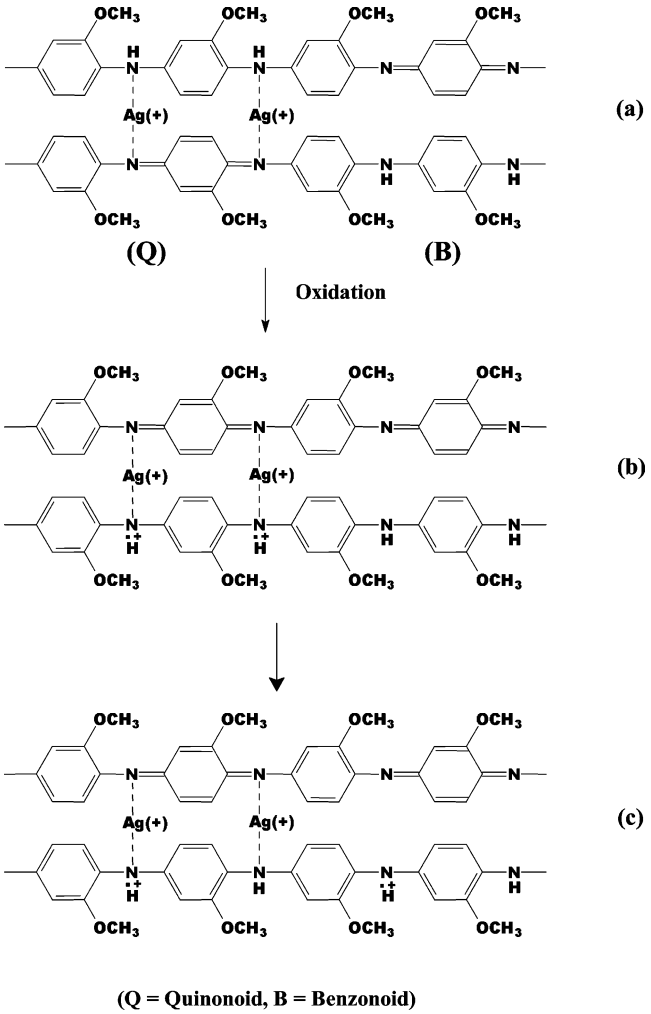

blue shift in the UV−vis spectra. After the doping of POMA is complete, it forms a hybrid with DNA through electrostatic interaction between its radical cation and DNA anion.[44−46] The silver atoms produced in this reaction become stabilized by the DNA, forming Ag nanoparticles.[5,52] After the formation of the POMA−DNA hybrid, POMA undergoes a slow uncoiling process on the DNA surface due to the repulsive interaction of adjacent radical cations of doped POMA.[44−46] As a result, the conjugation length of POMA increases, producing a slow red shift of the π band to polaron band transition peak of UV−vis spectra. At about 7−8 days, it reaches equilibrium and a leveling of the π band to polaron band transition peak occurs.

Support for the above mechanism may be furnished from the conductivity data, which are in the same order as that of the pure POMA−DNA hybrid at the same composition (W_{DNA} = 0.71).[45] The same conductivity value suggests that in the POMA doping is taking place by Ag^+. Also, the UV−vis spectra approximately support the above mechanism from the fluctuation of the π band to polaron band transition and polaron band to π^* band transition peaks at the initial level of aging. The slow continuous red shift of the π band to polaron band transition after 53 h of aging is due to the uncoiling of POMA chain attached to the DNA surface.[44−46] Because of the polyanionic character of DNA, it acts as a good stabilizer of nanoparticles and no agglomeration of Ag nanoparticles takes place. When the experiment was repeated without DNA, agglomerated Ag particles are immediately produced. Also, the increased concentration of quinonoid structure in the POMA chain, as evidenced from FT-IR spectra, supports the above mechanism, because the above mechanism proposes a larger amount of quinonoid structure formation. Thus, the formation of Ag nanoparticle is a redox process where Ag^+ is reduced to metallic Ag and POMA (EB) is oxidized into the POMA (PB) form.

Conclusion

It may be concluded that a novel silver nanocomposite of conducting polymer−DNA hybrid has been successfully prepared by adding DNA (Na-salt) solution to a POMA (EB) and $AgNO_3$ mixture solution. This material may have utility in various biosensing appliances. The conformation and crystal structure of DNA remain intact during the nano-biocomposite formation. Interesting UV−vis spectra are observed in the complex, showing an initial fluctuation of the π band to polaron band transition peak followed by a slow red shift with time due to the uncoiling of POMA chain on the DNA template. The dc conductivity value of the hybrid nanocomposite is almost the same as that of the pure POMA−DNA hybrid at the same composition, but the I−V characteristic curve is somewhat different, showing a long range of insulating region on low applied voltage. However, at higher applied voltage, it shows the property of large band gap semiconducting material.

Acknowledgment. We gratefully acknowledge the help extended by Bose Institute, Kolkata, for CD measurements. A.D. also acknowledges the Council of Scientific and Industrial Research, New Delhi, for granting a research fellowship.

Supporting Information Available: Figures showing I−V characteristic curves of Ag-nano-biocomposite and FTIR spectra of freeze-dried samples of POMA/$AgNO_3$ and Na-DNA/$AgNO_3$ mixtures. This material is available free of charge via the Internet at http://pubs.acs.org.

References and Notes

(1) Petty, J. F.; Zheng, J.; Hud, N. V.; Dickson, R. M. *J. Am. Chem. Soc.* **2004**, *126*, 5207.
(2) Deng, Z.; Mao, C. *Nano Lett.* **2003**, *3*, 545.
(3) Monson, C. F.; Woolley, A. T. *Nano Lett.* **2003**, *3*, 359.
(4) Becerril, H. A.; Stoltenberg, R. M.; Monson, C. F.; Woolley, A. T. *J. Mater. Chem.* **2004**, *14*, 611.
(5) Wei, G.; Zhou, H.; Liu, Z.; Song, Y.; Wang, L.; Sun, L.; Li, Z. *J. Phys. Chem. B* **2005**, *109*, 8738.
(6) Braun, E.; Eichen, Y.; Sivan, U.; Ben-Yoseph, G. *Nature* **1998**, *391*, 775.
(7) Seidel, R.; Colombi Ciacchi, L.; Weigel, M.; Pompe, W.; Mertig, M. *J. Phys. Chem. B* **2004**, *108*, 10801.
(8) Richter, J.; Seidel, R.; Kirsch, R.; Mertig, M.; Pompe, W.; Plaschke, J.; Schackert, H. K. *Adv. Mater.* **2000**, *12*, 507.
(9) Qin, W. J.; Yung, L. Y. L. *Langmuir* **2005**, *21*, 11330.
(10) Wei, Y.; Yeh, J.-M.; Wang, W.; Jang, G.-W. U.S. Patent 5,868,-966, 1999.
(11) Tian, S. J.; Liu, J. Y.; Zhu, T.; Knoll, W. *Chem. Commun.* **2003**, *21*, 2738.
(12) Tian, S. J.; Liu, J. Y.; Zhu, T.; Knoll, W. *Chem. Mater.* **2004**, *16*, 4103.
(13) Khanna, P. K.; Singh, N.; Charan, S.; Viswanath, A. K. *Mater. Chem. Phys.* **2005**, *92*, 214.
(14) Kitani, A.; Akashi, T.; Sugimoto, K.; Ito, S. *Synth. Met.* **2001**, *121*, 1301.
(15) Coutanceau, C.; Croissant, M. J.; Napporn, T.; Lamy, C. *Electrochim. Acta* **2001**, *46*, 579.
(16) Lai, E. K. W.; Beatttie, P. D.; Holdcroft, S. *Synth. Met.* **1997**, *84*, 87.
(17) Maksimov, Y. M.; Kolyadko, E. A.; Shishlova, A. V.; Podlovchnko, B. I. *Russ. J. Electrochem.* **2001**, *37*, 777.
(18) Drelinkiewicz, A.; Hasik, M.; Kloc, M. *Catal. Lett.* **2000**, *64*, 41.
(19) Josowicz, M.; Li, H.-S.; Domansky, K.; Baer, D. R. *Electroanalysis* **1999**, *11*, 10.

(20) Kinyanjui, J. M.; Hatchett, D. W.; Smith, J. A.; Josowich, M. *Chem. Mater.* **2004**, *16*, 3390.
(21) Pinter, E.; Patakfalvi, R.; Fulei, T.; Gingl, Z.; Dekany, I.; Visy, C. *J. Phys. Chem. B* **2005**, *109*, 17474.
(22) Suri, K.; Annapoorni, S.; Tandon, R. P. *Bull. Mater. Sci.* **2001**, *24*, 563.
(23) Ferreira, M.; Zucolotto, V.; Huguenin, F.; Torresi, R. M.; Oliveira, O. N. *J. Nanosci. Nanotechnol.* **2002**, *2*, 29.
(24) Malik, S.; Btabyal, S.; Basu, C.; Nandi, A. K. *J. Mater. Sci. Lett.* **2003**, *22*, 1113.
(25) Henry, M. C.; Hsueh, C.-C.; Timko, B. P.; Freund, M. S. *J. Electrochem. Soc.* **2001**, *148*, D155.
(26) Zhou, Y.; Itoh, H.; Uemura, T.; Naka, K.; Chujo, Y. *Langmuir* **2002**, *18*, 277.
(27) Liu, Y.-C.; Chuang, T. C. *J. Phys. Chem. B* **2003**, *107*, 12383.
(28) Mirkin, C. A.; Letsinger, R. L.; Mucic, R. C.; Storhoff, J. J. *Nature* **1996**, *382*, 607.
(29) Nam, J. M.; Thaxton, C. S.; Mirkin, C. A. *Science* **2003**, *301*, 1884.
(30) Liu, J.; Gomez-Kaifer, M.; Kaifer, A. E. *Structure and Bonding*; Springer: Berlin, 2001.
(31) Andres, R. P.; Bein, T.; Dorogi, M.; Feng, S.; Henderson, J. I.; Kubiak, C. P.; Mahoney, W.; Osifchin, R. G.; Reifenberger, R. *Science* **1996**, *272*, 1323.
(32) El-Sayed, M. A. *Acc. Chem. Res.* **2001**, *34*, 257.
(33) Maier, S. A. *Adv. Mater.* **2001**, *13*, 1501.
(34) Kamat, P. V. *J. Phys. Chem. B* **2002**, *106*, 7729.
(35) Valden, M.; Lai, X.; Goodman, D. W. *Science* **1998**, *281*, 1647.
(36) Tian, Z. Q.; Ren, B.; Wu, D. Y. *J. Phys. Chem. B* **2002**, *106*, 9463.
(37) Pradhan, N.; Pal, A.; Pal, T. *Colloids Surf., A* **2002**, *196*, 247.
(38) Nakatsuji, H.; Nakai, H.; Ikeda, K.; Yamamoto, Y. *Surf. Sci.* **1997**, *384*, 315.
(39) Zhang, Z. Q.; Patel, R. C.; Kothari, R.; Johnson, C. P.; Friberg, S. E.; Aikens, P. A. *J. Phys. Chem. B* **2000**, *104*, 1176.
(40) Manna, A.; Imae, T.; Iida, M.; Hisamatsu, N. *Langmuir* **2001**, *17*, 6000.
(41) Xue, B.; Chen, P.; Hong, O.; Lin, J. Y.; Tan, K. L. *J. Mater. Chem.* **2001**, *11*, 2378.
(42) Ahmad, A.; Mukherjee, P.; Senapati, S.; Mandal, D.; Khan, M. I.; Kumar, R.; Sastry, M. *Colloids Surf., B* **2003**, *28*, 313.
(43) Drimitreiv, O. P. *Macromolecules* **2004**, *37*, 3388.
(44) Dawn, A.; Nandi, A. K. *Macromol. Biosci.* **2005**, *5*, 441.
(45) Dawn, A.; Nandi, A. K. *Macromolecules* **2005**, *38*, 10067.
(46) Dawn, A.; Nandi, A. K. *Langmuir* **2006**, *22*, 3273.
(47) Roy, B.; Chakravorty, D. *J. Phys.: Condens. Matter* **1990**, *2*, 9323.
(48) Xia, Y.; Wiesinger, J. M.; MacDiarmid, A. G.; Epstein, A. J. *Chem. Mater.* **1995**, *7*, 443.
(49) Stejskal, J.; Kratochvil, P.; Radhakrishnan, N. *Synth. Met.* **1993**, *61*, 225.
(50) Huang, W. S.; MacDiarmid, A. G. *Polymer* **1993**, *34*, 1833.
(51) Kumbhar, A. S.; Kinnan, M. K.; Chumanov, G. *J. Am. Chem. Soc.* **2005**, *127*, 12444.
(52) Berti, L.; Alessandrini, A.; Facci, P. *J. Am. Chem. Soc.* **2005**, *127*, 11216.
(53) (a) Palaniappan, S.; Nivasu, V. *New J. Chem.* **2002**, *26*, 1490. (b) Tang, J.; Jing, X.; Wang, B.; Wang, F. *Synth. Met.* **1988**, *24*, 231. (c) Salaneck, W. R.; Liedberg, B.; Inganas, O.; Erlandsson, R.; Lundstrom, I.; MacDiarmid, A. G.; Halpern, M.; Somasiri, N. L. D. *Mol. Cryst. Liq. Cryst.* **1985**, *121*, 191. (d) Zengin, H.; Zhou, W.; Jin, J.; Czerw, R.; Smith, D. W., Jr.; Echegoyen, L.; Carroll, D. L.; Foulger, S. H.; Ballato, J. *Adv. Mater.* **2002**, *14*, 1480.
(54) (a) Hatchett, D. W.; Josowicz, M.; Janata, J. *J. Phys. Chem. B* **1999**, *103*, 10992. (b) Stejskal, J.; Trchova, M.; Prokes, J.; Sapurina, I. *Chem. Mater.* **2001**, *13*, 4083. (c) Qiu, H.; Wan, M.; Matthews, B.; Dai, L. *Macromolecules* **2001**, *34*, 675. (d) Garai, A.; Kuila, B. K.; Nandi, A. K. *Macromolecules* **2006**, *39*, 5410.
(55) Higuchi, M.; Imoda, D.; Hirao, T. *Macromolecules* **1996**, *29*, 8277.
(56) The formation of the Ag−POMA complex may be evidenced from the FT-IR spectra (Supporting Information Figure 2). After the mixture of POMA and $AgNO_3$ solution (mixed for 8 h) was dried, the N═Q═N stretching vibration band[53] shows a shift to higher energy (1115 to 1122 cm^{-1}). It may be due to the complexation of the above nitrogen with Ag^+ making the N═Q═N stretching vibration difficult and shifting the band to higher energy. Also, the deformation vibration of quinonoid ring shifts to lower energy (1589 to 1579 cm^{-1}) because of lowering of C═N bond order due to the complex formation with Ag^+. The FT-IR spectra of the mixture of Na−DNA−$AgNO_3$ solution (mixed for 8 h) do not exhibit any substantial change in the 1061 and 1226 cm^{-1} peaks (for C−O−P sugar−phosphate and asymmetric phosphate group vibration, respectively), indicating retention of B conformation of DNA.[57] Thus, POMA is playing a major role in the silver nanoparticle formation in the nano-biocomposite. The 1382 cm^{-1} peak in both of the spectra of Supporting Information Figure 2 is for asymmetric $-NO_3$ stretching.[58]
(57) Hackl, E. V.; Blagoi, Y. P. *Acta Biochim. Pol.* **2000**, *47*, 103.
(58) Colthup, N. B.; Daly, L. H.; Wiberley, S. E. *Introduction to Infrared and Raman Spectroscopy*; Academic Press: New York, 1964; p 287.